Optimal design of integrally gated CNT field-emission devices using a genetic algorithm

2007 Nanotechnology 18 395203

(http://iopscience.iop.org/0957-4484/18/39/395203)

Nanotechnology **18** (2007) 395203 (10pp) doi:10.1088/0957-4484/18/39/395203

Optimal design of integrally gated CNT field-emission devices using a genetic algorithm

P Y Chen[1], C H Chen[2], J S Wu[3], H C Wen[4] and W P Wang[3]

[1] National Nano-Device Laboratories, Science-Based Industrial Park, Hsinchu 30078, Taiwan
[2] Department of Computer Science, National Chiao Tung University, Hsinchu 30050, Taiwan
[3] Department of Mechanical Engineering, National Chiao Tung University, Hsinchu 30050, Taiwan
[4] Department of Mechanical Engineering, National Chung Cheng University, Chiayi 621, Taiwan

E-mail: pychen@mail.ndl.org.tw

Received 1 May 2007, in final form 26 July 2007
Published 4 September 2007
Online at stacks.iop.org/Nano/18/395203

Abstract
A method to optimize the focusing quality of integrally gated CNT field-emission (FE) devices by combining field-emission modeling and a computational intelligence technique, genetic algorithm (GA), is proposed and demonstrated. In this work, the e-beam shape, as a characteristic parameter of electron-optical properties, is calculated by field-emission simulation modeling. Using a design tool that combines GA and physical modeling, a set of structural and electrical parameters for four FE device groups, including double-gate, triple-gate, quadruple-gate and quintuple-gate type, were optimized. The resultant FE devices exhibit satisfactory e-beam focusabilities and the extracted parameters with the best performance for each type of FE device were represented to be fabricated by a VLSI technique. The GA-based automatic design parameter extraction will significantly benefit the design of integrated electron-optical systems for versatile vacuum micro- and nano-electronic applications.

1. Introduction

Field emission is one of the most fascinating properties of carbon nanotubes (CNTs) and has attracted extensive studies of its fundamental understanding both in the fields of physics and chemistry [1–3]. In addition, possible applications in field-emission display (FED), high-frequency microwave amplifier, x-ray source and electron microscopy, among others [4–11], have also prompted numerous studies in the past decade. Due to modern nanofabrication techniques such as the chemical vapor deposition (CVD) [4, 5] and screen-printing [6–8] methods, films consisting of vertically aligned CNTs or single CNT emitters [1] could be grown within the patterned area and could be further integrated to gated vacuum micro- and nano-electronic devices. For a typical gated FE triode, as shown in figure 1(a), a CNT thin film as a collective emitter is located below the center of the extraction gate. As the extraction gate is biased to a large enough positive voltage with respect to the emitter, electrons at the surface of the CNT thin film are first emitted into the vacuum via quantum tunneling through a solid–vacuum potential barrier, and then are accelerated to the anode. One of the most critical design issues is how to reduce the spreading diameter of electrons arriving at the anode, while keeping the required amount of emission current. To enhance the e-beam focusability, one [6–8, 11] or several [12] coaxial focusing gates, serving as electrostatic lenses to focus the electron trajectories, are stacked above the extraction gate and separated by an insulating layer (SiO_2, $\varepsilon_{ox} = 3.9$) in between. For example, figure 1(b) shows a typical quadruple-gate FE device. Since there are many design parameters, such as configurations of gate geometry and biased potentials, which can significantly influence the focusing capability of the e-beam, an effective optimal design tool for complicated FE devices is strongly needed. Field-emission simulations have become an indispensable technique for the practical design of various FE devices [6–15]. However, most studies on FE device design focused on the optimization of either only

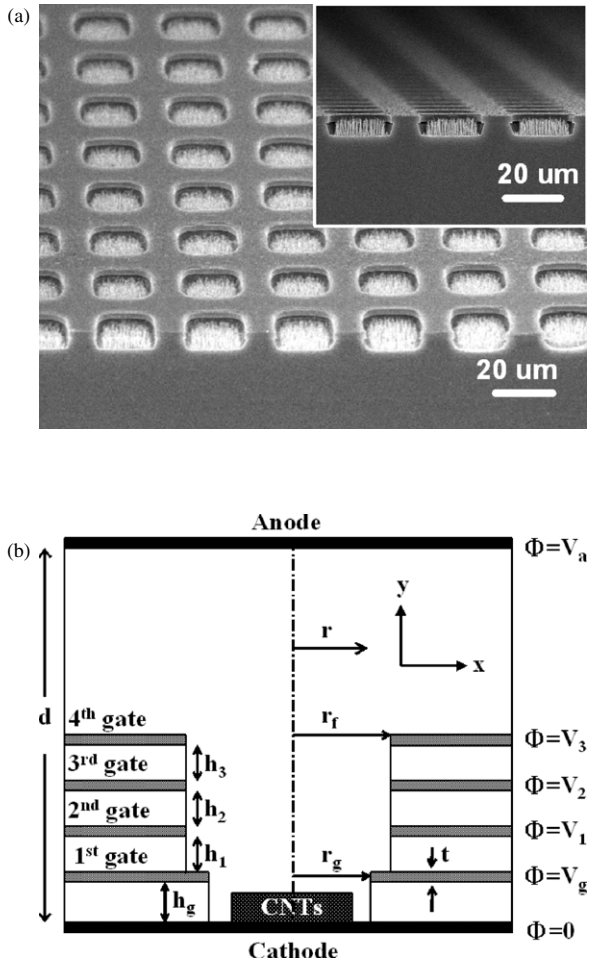

Figure 1. (a) SEM images of the FE triode; CNT thin films are fabricated by a direct growth method using chemical vapor deposition (CVD) and gate configurations are patterned by lithography; (b) electrical and structural parameters of a quadruple-gate FE device under optimization.

one of the system parameters [11, 12], developing a new architecture [13, 14], or a new operational mode [10, 11, 15] of the gate electrodes. To the best knowledge of the authors, no work has been done on applying a global optimization scheme for designing FE devices, where all design parameters underwent the optimization process simultaneously.

In this paper, we have proposed the optimization of integrally gated FE devices by genetic algorithm (GA), as promoted by Holland and his colleagues [16], which is one of the computational intelligence techniques. GA have been successfully implemented in various academic research work and industrial applications, such as communications [17], photonics [18–20] and advanced VLSI technology [21]. GA is a stochastic optimization technique based on the biological principles of natural selection and evolution. It is well suited for complex problems such as the present one, in which a number of system parameters must be optimized simultaneously, and some other practical problems which may not have a unique, well-defined optimum. In this work, we intended to adapt the GA to the field of electron optics, in which optimal design of the gated FE device could be easily achieved.

In brief summary, we carried out GA optimization for double-gate [6–8], triple-gate, recently proposed quadruple-gate [12] and FE devices. A typical FE triode (single-gate) without any auxiliary focusing gate is also simulated. In section 2, we will briefly describe the implementation of a parallel-scheme GA for e-beam focusability optimization. This proposed GA can be easily extended to other applications in the field of electron optics, which is often involved with many electrical, magnetic and structural parameters.

2. Numerical methods

In this section, the implementation of the proposed GA is described, including the problem definition, the principle of the GA and the evaluation of the engineering- and physical-based fitness function. In each part, detailed procedures and specific algorithms are provided.

2.1. Problem definition and encoding method

How to determine the structural and electrical parameters of the electron-optical system to perform the optimization is an important subject. For the FE devices in this work, we can obtain the satisfactory performance by adjusting the position and biased voltage of the integrated focusing gates which are the most important ones in controlling the quality of e-beam focusability. Take the quadruple-gate type shown in figure 1(b) for example: the e-beam trajectories depend on the position and bias voltage of the focusing gates: $\mathrm{traj}(x, y, z) = \mathrm{traj}(h_1, h_2, h_3, V_1, V_2, V_3)$. The variable parameters in an optimization problem form the components of a parameter vector; all possible parameter vectors (here $\vec{h} = (h_1, h_2, \ldots, h_n)$; $\vec{V} = (V_1, V_2, \ldots, V_n)$) constitute a multidimensional search space. In GA, each component of the search argument vector is regarded as one gene. Therefore, in the quadruple-gate type, six genes (h_1, h_2, h_3, V_1, V_2 and V_3) are combined into one chromosome of an individual. Following the same rule, the chromosome of an individual for double-gate, triple-gate and configuration contains two genes (h_1 and V_1), four genes (h_1, h_2, V_1, and V_2) and eight genes (h_1, h_2, h_3, h_4, V_1, V_2, V_3, and V_4), respectively. Each gene stands for a variable parameter of FE devices and is encoded as a binary string G:

$$G = \frac{1}{2^{N-1}} \sum_{n=0}^{N-1} 2^n \, b_n, \tag{1}$$

where b_n is the binary bit in the nth point along the gene and N is the total length of each gene (number of binary-coded digits). This binary string G in the chromosome space is then mapping to the corresponding variable P in the parameter space by a decoding process:

$$P = P_{\min} + G \times (P_{\max} - P_{\min}) \tag{2}$$

where $G \in \{0, 1\}$, P represents all parameters to be extracted, and $P_{\min}$ and $P_{\max}$ are the initial setting of maximum and minimum value of device variables. In such a manner, GA operated on a discretized coding of the parameters rather than the parameters themselves. Each parameter consists of 8 bits and thus the length of the whole chromosome for double-gate,

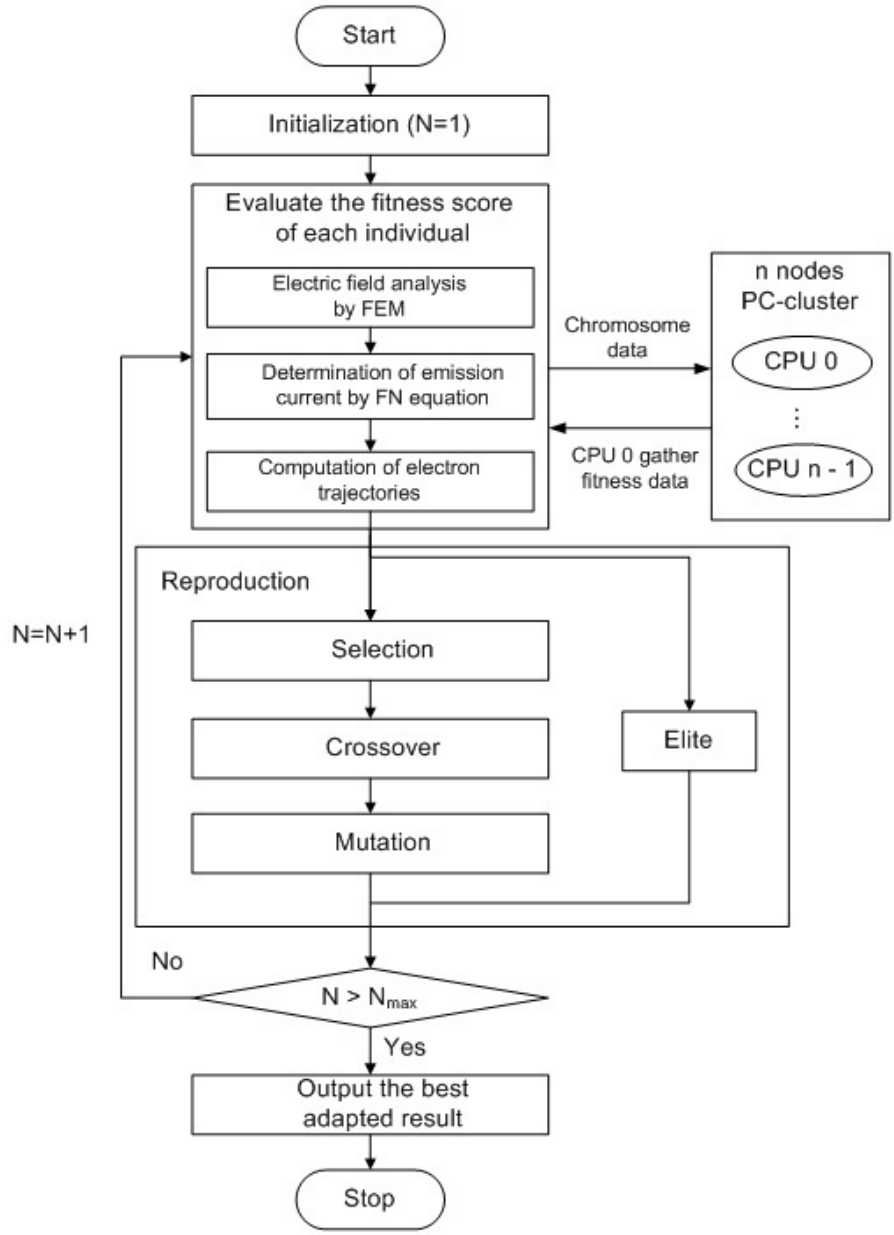

Figure 2. Flowchart of GA used for the optimization design of integrated FE devices.

triple-gate, quadruple-gate and types are 16, 32, 48 and 64 bits, respectively.

The fixed parameters used in this work include: 30 μm and 40 μm for radius of the extraction gate (r_g) and the focusing gate (r_f), respectively; 0.2 μm for thickness of the gate electrodes (t); 200 μm for the anode-to-cathode distance (d). Typically, the applied anode-to-cathode electric field strength is in the range of 2–6 V/μm [10], while the applied biased voltage at the extraction gate is in the range of 60–80 V to extract enough emission current for the operation of FE devices [6–8]. In this work, the applied voltage at anode and at extraction gate (1st gate) is set to 900 V and 80 V, respectively, with respect to the anode-to-cathode separation of 200 μm. It should be noted that, in order to avoid electrical breakdown and the arc problem between two gate electrodes [22], the range of adjustable parameters should be taken carefully. The searching area, which is the extent of the design parameters, is defined and summarized in table 1.

2.2. *Principle of genetic algorithms*

Figure 2 shows a flowchart of the GA optimization process adopted in the present study. At the start of the GA, the initial values of G in each gene are randomly generated between 0 and 1 with uniform probability. N_C individuals (here N_C = 40) are randomly generated to establish the initial population. Each individual is assigned a fitness value, which provides an indication of solutions which are the most probable to evolve towards a better next generation. Thus, a set of trial solutions can be randomly generated and then evolved toward

Table 1. Searching areas for each parameter in GA analysis.

	Double-gate type	Triple-gate type	Quadruple-gate type	Quintuple-gate type
h_1 (μm)	1–3.5	1–3.5	1–3	1–3
V_1 (V)	−50–50	−50–50	−50–50	−50–50
h_2 (μm)	N/A	1–3	1–3	1–3
V_2 (V)	N/A	−50–50	−50–50	−50–50
h_3 (μm)	N/A	N/A	0.5–2.5	0.5–2.5
V_3 (V)	N/A	N/A	−50–50	−50–50
h_4 (μm)	N/A	N/A	N/A	0.5–2.5
V_4 (V)	N/A	N/A	N/A	−50–50

the optimal solution under the pressure of the fitness function. The fitness of an individual is defined as the e-beam diameter on the anode ($D_{\text{e-beam}}$). To evaluate the e-beam diameter, a field-emission simulation modeling was developed and details are to be discussed in section 2.3. Based on the fitness function, the next generation is produced by the 'reproduction' process utilizing the biologically analogous operators of *selection*, *crossover* and *mutation*, as shown in figure 2. In production, a pair of individuals is selected from the current population to act as the parents. The parents undergo crossover and mutation with probability p_c and p_m, respectively, which in turn creates a pair of new individuals as 'children'. The operation steps of production are summarized as follows:

(i) *Selection*: This procedure utilizes the fitness of a given individual to determine which individuals are fit enough to remain in the population. We employ the *roulette-wheel* selection [17] for the stochastic-selection strategy, in which individuals are selected based on the probability of selection p_s given by

$$p_s = f_i \Big/ \sum_{i=1}^{N_C} f_i, \tag{3}$$

where f_i is the fitness of the ith individual. It is to be noted that the probability of selecting one individual from N_C individuals in a population is a function of the relative fitness of the individuals. This means that the individuals with higher fitness value are more likely to be selected as the parents for generating new individuals (children).

(ii) *Crossover*: Once the parent is selected, the two chromosomes undergo crossover with a probability of crossover $p_c = 0.7$, which is reported as the optimal value. Here, a two-point crossover method is employed. Crossover is carried out by exchanging equivalent segments of the chromosomes by means of randomly choosing points to produce two new chromosomes. The purpose of crossover is to rearrange the genes, with the objective of creating better combinations of genes to result in fitter individuals.

(iii) *Mutation*: Mutation is also necessary to maintain the diversity in the population and explore the solutions which are not yet present, thus preventing quick convergence to a local minimum. Mutation is usually performed by randomly altering an individual gene with the probability of mutation $p_m = 0.05$. In the case of binary coding, it means to randomly select a bit from the chromosome string and invert it. In other words, '1' becomes '0' and vice versa. These children are then placed in the new generation. It is to be noted that the elitist strategy is employed in this paper, in which the top 2% chromosomes defined as the 'elite chromosomes' from the preceding generation are preserved and directly inserted into a new generation. This procedure can ensure the 'elite' of each population survive to be used as parents in the next population. Therefore, the elite chromosomes can reproduce more often than the non-elite ones. These processes, including selection, crossover and mutation, are repeated until the size of the new generation is the same as the current generation.

The GA processes are iterated until 40 generations are calculated and then we save the best chromosome in each generation. After the ending of GA flow, the parameters encoded in the chromosome with the best fitness are converted into floating point numbers and then mapped to the parameter space according to equations (1) and (2). Most of the steps used in this paper are commonly used in a GA regardless of the problem being solved, except that a parallel scheme of evaluating the fitness on a eight-node PC-cluster system is introduced to speed up the time of the GA evolution, which will be introduced later.

2.3. Fitness function

To obtain the e-beam diameter related to the fitness of an individual, a physical modeling for simulating field-emission properties was developed based on the following steps: (1) solving the electrostatic characteristics, (2) determining field emission from a CNT thin film by Fowler–Nordheim (FN) law, and (3) tracing the motion of electrons to obtain the electron trajectories. The above steps are described in detail in the following in turn.

First, the electrostatic distributions of the corresponding structures generated by the GA are obtained by solving Poisson's equation. Since the space–charge effect is neglected, the Poisson equation reduces to the Laplacian equation as

$$\nabla^2\phi = \frac{\partial^2\phi}{\partial x^2} + \frac{\partial^2\phi}{\partial y^2} = 0, \tag{4}$$

where ϕ is the electric potential. The Laplacian equation is solved using the finite-element method (FEM) [23]. After calculating the potential distribution, the electric field distribution can be derived by numerically differentiating the potential with respect to Cartesian coordinates. Then,

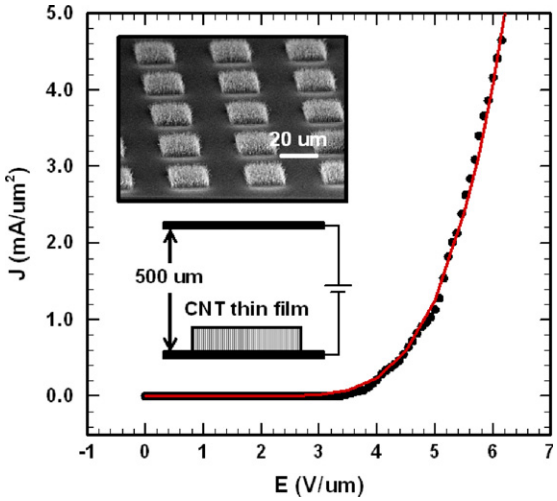

Figure 3. Measured J–E data (●) and the calculated results ((red) solid line) using the parameters: $A = 6.84$ (mA/(V/μm)^2) and $B = 24.80$ (V/μm); the inset is the patterned CNT thin film and the schematics of the diode-type FE measurement.

the emission current density from the cathode surface was determined by the modified Fowler–Nordheim (FN) equation:

$$J = AE^2 \exp\left(-\frac{B}{E^2}\right) \tag{5}$$

where E is the electric field around the emission surface, and A and B are the emission parameters, which are empirical parameters related to the work function of the material and field enhancement factor. It is practically impossible to consider the detailed morphology of all CNT emitters in the modeling. In this work, CNT forests are treated as a single emission layer that is an equivalent thin film with a width of 20 μm and a thickness of 3 μm, which is in accordance with the observed SEM image. In the macroscale simulation at device level, the CNT forest was usually treated as a thin film (slab) to simplify the difficulty of the modeling [10]. The empirical emission parameters of the CNT thin film were then obtained by fitting the simulation to the experimental data. It is believed to be more realistic and proper to use the experimental data for calibration. Figure 3 shows the measured FE characteristics of the patterned CNT thin film by a typical diode-type measurement, in which the inset is the SEM image of the patterned CNT thin film grown on a silicon substrate by the CVD method. Using the experimental data, the emission parameters of the CNT thin film are calibrated as $A = 6.84 \times 10^{-2}$ (A/(V/μm)^2) and $B = 24.80$ (V/μm) by fitting equation (5) to the measured data. These two calibrated coefficients are then kept the same in the numerical modeling for all types of FE devices in the present study. This method can effectively simplify the modeling without loss of generality, which was adopted in most FE-device-related simulation studies (e.g. [10]). Once the electric field around the CNT thin film in the gated FE device is calculated, the emission current density can be roughly estimated. The emission current from the emitter surface is determined by the integral of the current density (equation (5)) using the local value of the electric field at the surface of the CNT thin film. Finally, the electron trajectories are calculated according to the equation of motion (Lorentz equation) using the fourth-order Runge–Kutta method [14] for time integration. Emitted electrons from the CNT thin film are then traced toward the anode based on the electric field obtained from an electrostatic Laplacian equation. From the simulated electron trajectories, the beam spot size on the anode, which represents the value of fitness in GA, can be obtained as

$$\text{Fitness} = F(h_1, V_1; \cdots, h_n, V_n) = D_{\text{e-beam}} = 2 \times \frac{\int_0^\infty J(r) r 2\pi r \, \mathrm{d}r}{\int_0^\infty J(r) 2\pi r \, \mathrm{d}r}, \tag{6}$$

where $J(r)$ is the electron current density on the anode and r is the radial distance from the symmetric axis. Simulations

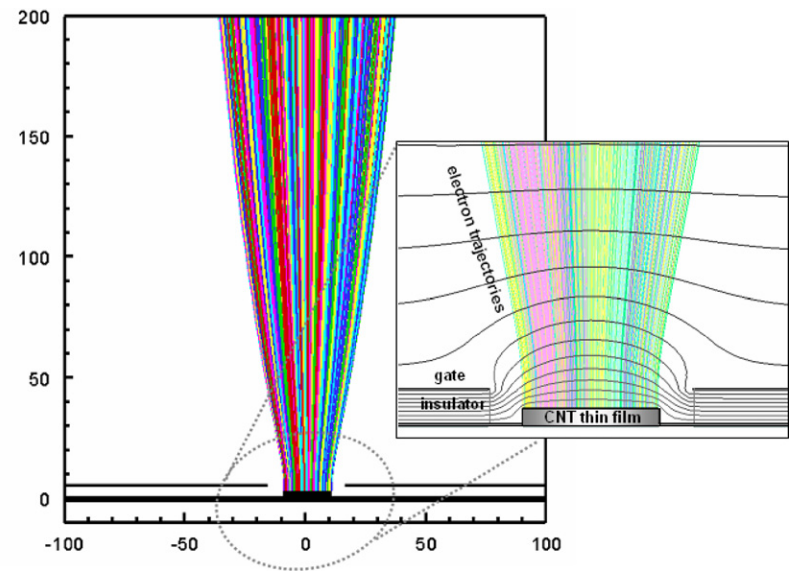

Figure 4. Electron trajectories of the FE triode; the enlarged picture is the potential distribution and electron trajectories near the extraction gate aperture.

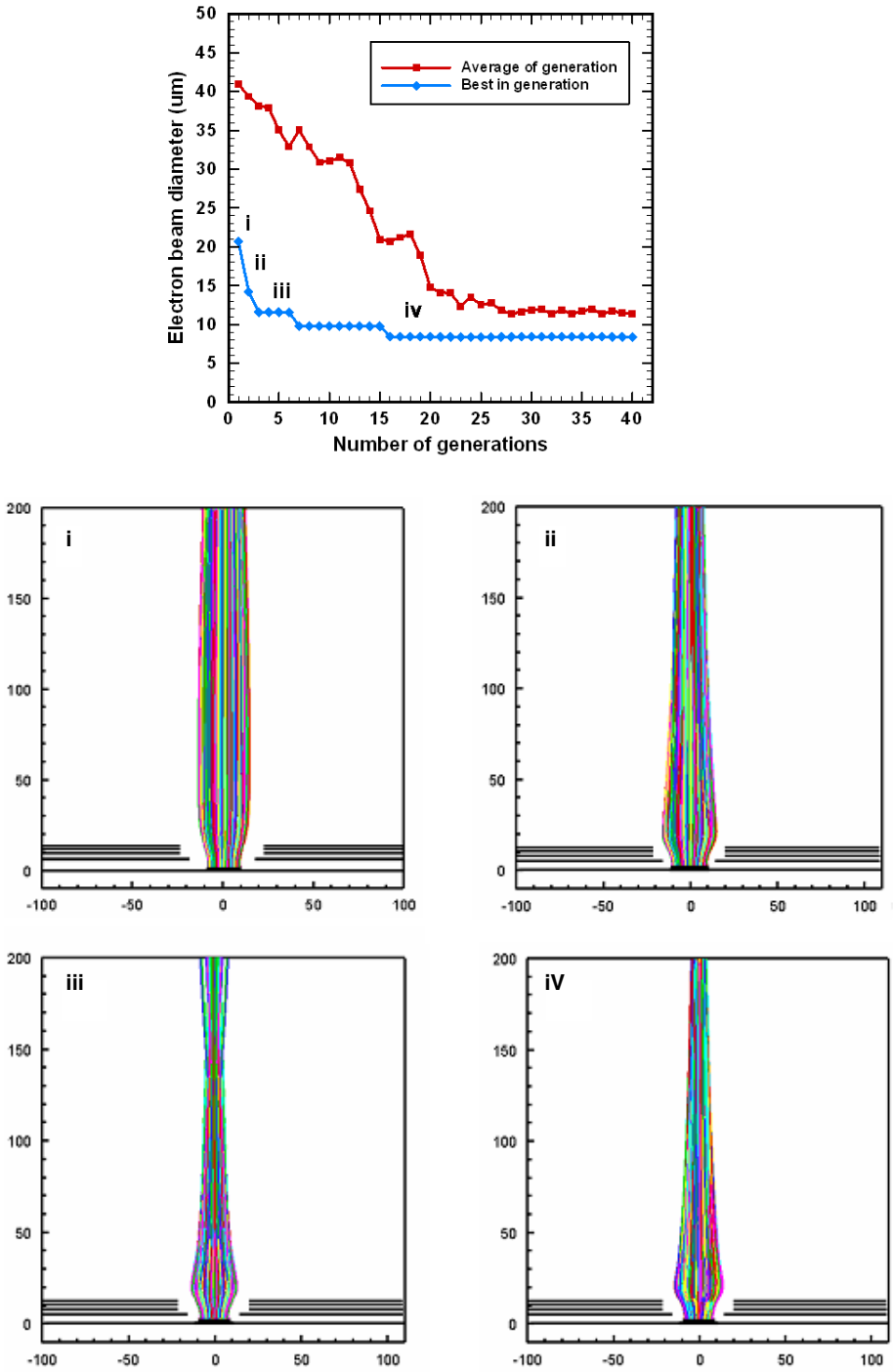

Figure 5. The best and average performance plotted as a function of generation (top). The unit cells show the best performance at different generations during the evolution process of GA (bottom).

of field emission are incorporated in a package that is used to evaluate the fitness function, which is the only connection between the physical problem and GA.

2.4. Parallel processing for a genetic algorithm

In contrast to the huge computational time for the physical modeling, only a relatively small portion of the time is spent in this part of the GA. For example, 1600 runs of the field-emission simulation are necessary for 40 individuals evolving over 40 generations. To reduce the computational time to an acceptable level, a parallel scheme for the GA is introduced to accelerate the evolution. Field-emission simulations for N_C individuals in one population are equally assigned to eight processors of a PC-cluster system, which results in only $N_C/8$ individuals being treated in each processor. Thus, fitness functions of individuals in the same population are separately

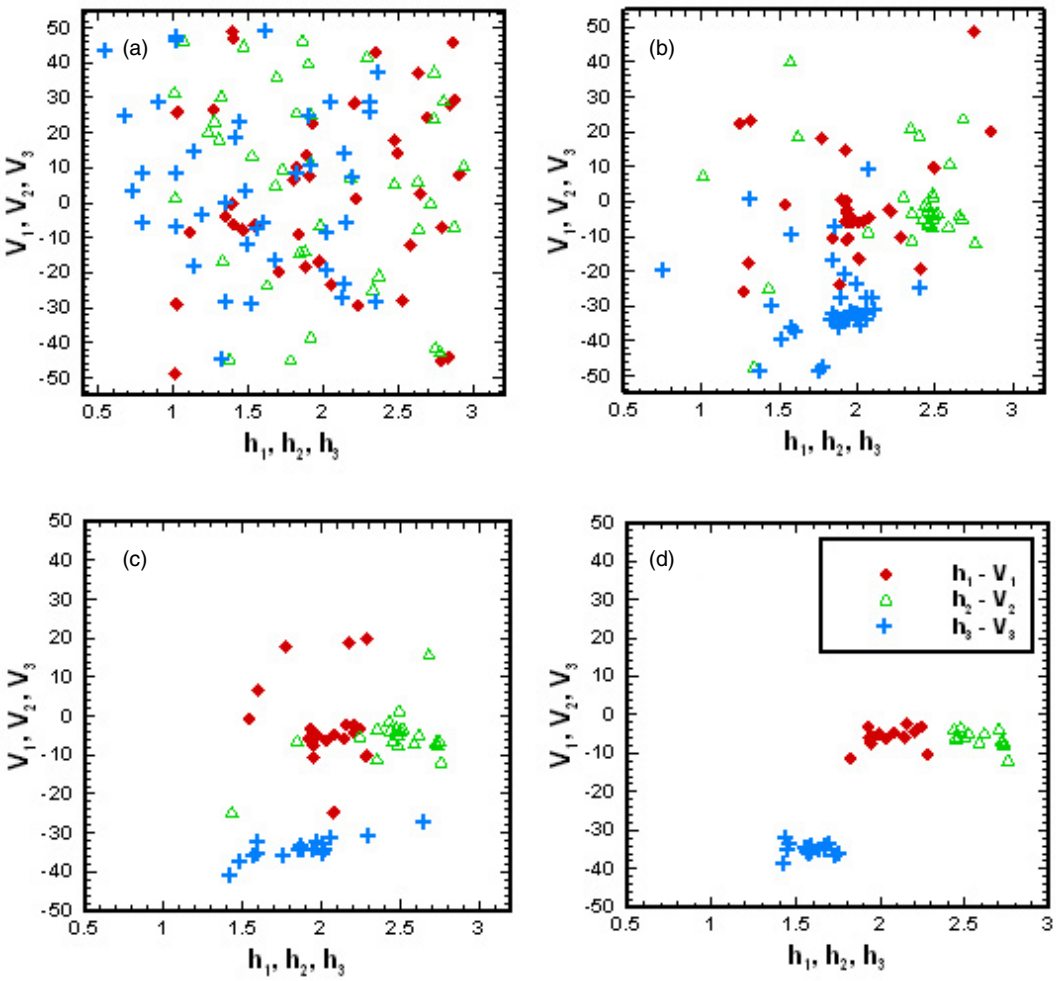

Figure 6. Population distributions (h_1–V_1 (◆), h_2–V_2 (△), h_3–V_3 (+)) of all individuals during the GA search process: (a) initial, (b) 10th, (c) 15th and (d) 30th generation. The optimal parameters are finally constrained in groups in the search space.
(This figure is in colour only in the electronic version)

evaluated from eight processors and are then gathered into the master processor for determining the next reproduction process.

3. Results and discussions

Figure 4 shows the e-beam shape of a typical FE triode without any auxiliary focusing electrodes and the exploded view is the magnified electron trajectories along with the potential distribution near the gate aperture. It is found that the emitted electrons diverge in vacuum space, leading to an undesirably large e-beam spot at the anode. In this case, the e-beam diameter on the anode is calculated as 65.126 μm. Therefore, an effective electrostatic focusing system is required to reduce the spot size of impinging electrons at the anode. In the present study, the four different types of focusing gates are vertically integrated in the FE triode to achieve this goal. Corresponding structural and electrical parameters of the four types of FE devices can then be automatically optimized by the proposed GA. Take the quadruple-gate type, for instance: figure 5 shows the peak and average progress of the GA optimization as a function of the number of generations. It is seen that both values converge to a minimum eventually. The corresponding e-beam shape of the best fitness at different generations during the evolution processes are shown at the bottom of figure 5. We can find a good evolution behavior is presented as well as the optimal e-beam shape after convergence. Upon completion, the global optimized solution of the quadruple-gate type yields an e-beam diameter of 9.082 μm. Figure 6 shows the population distributions during the GA searching process. It is seen that the parameters of the initial population are randomly distributed (figure 6(a)), gradually converged (figures 6(b) and (c)) and finally constrained (figure 6(d)) at the end of the evolution process.

Table 2 summarizes the optimized design parameters extracted by GA and the corresponding e-beam diameters at the anode for double-gate, triple-gate, quadruple-gate and FE devices. The corresponding electron trajectories for each design are presented in figure 7. As compared to the FE triode, the optimized e-beam diameter for double-gate, triple-gate, quadruple-gate and types was reduced to 10.038 μm, 9.223 μm, 9.082 μm and 8.873 μm, respectively. It is clear that the extracted parameters for each type do not follow the same rule in obtaining the smallest e-beam diameter. This is because GA utilizes a parallel and adaptive

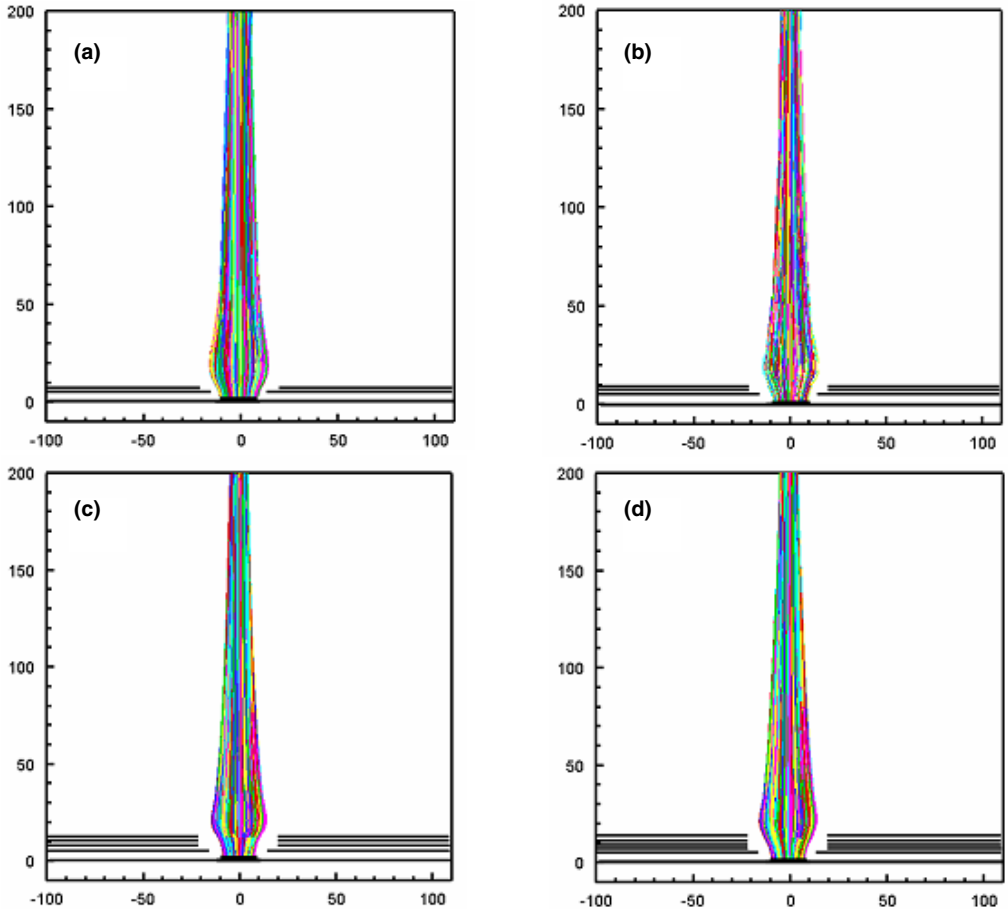

Figure 7. Optimized electron-beam focusing of (a) double-gate, (b) triple-gate, (c) quadruple-gate and (d) type of FE device.

search method in the optimization–design process. For each specific problem, GA may independently search its unique optimum in the parameter space. For making a comparison, optimization using one of the traditional methods, the gradient-based optimization [24, 25], has been done. The results are summarized in table 3. We can find that as the number of variables increases, the results were more likely to be trapped in the local minima region. This makes GA a very preferred choice for optimization of complex electron-optical problems. When the number of variables was not many (2–4), the calculation time for a gradient-based method was several hours; however, the calculation time increased with the increasing number of variables. For the quintuple-gate structure, the calculation time for a gradient-based method increased to 1.5 days, comparable to our parallel-scheme GA with eight CPU nodes (∼1.8 days). In this case, most of the calculation time was spent on the physical modeling rather than the optimization programming itself. Since no gradient is calculated, only the fitness function is evaluated and GA can allow more variables to be optimized at the same time than the traditional method can. Moreover, owing to the parallel search algorithm, GA optimization can be performed in a parallel scheme and the optimization speed of GA will be accelerated by increasing the number of CPU nodes. This makes GA a unique optimization method for physical problems with many variables.

Among the four types, type produces the smallest e-beam diameter; that is to say, type has the best e-beam focusability. This outcome is highly expected since more flexibility with increasing number of focusing gates is guaranteed for producing a reduced e-beam diameter. However, the triple-gate FE device is strongly recommended for practical design purposes, considering: (1) minor difference of the optimized smallest e-beam diameters among various types, (2) increasing difficulty in adding more numbers of focusing gates into the pre-formatted triode-gate type in a real fabrication process, and (3) increasing difficulty in operating FE devices with more gates (more power sources, cross-talk, etc.). Using the design parameters extracted by GA, triple-gate FE devices can be fabricated following the pre-formatted FE triode (figure 1(a)) by CVD and lithography processes.

In general, increasing population size may possibly further optimize the results. To test the effect of the population size on the optimized results, we have used two different sizes of population as compared to $N_C = 40$, 20 (fewer) and 100 (more), to simulate both the quadruple-gate and types. Because a larger population size can provide more abundant trial solutions at the start of a GA, the optimization search process can avoid being trapped in the local minimum. For $N_C = 100$, the converged results show 7.3% and 4.6% decreasing the e-beam diameter for quadruple-gate and quintuple-gate type, respectively, as compared to the case of $N_C = 40$. In contrast,

Table 2. Optimized structural and electrical parameters for four types of integrated CNT FE devices.

	Triode	Double-gate type	Triple-gate type	Quadruple-gate type	Quintuple-gate type
h_1 (μm)	N/A	2.422	1.117	2.211	1.570
V_1 (V)	N/A	42.578	−46.875	−3.906	−1.172
h_2 (μm)	N/A	N/A	1.710	2.726	1.453
V_2 (V)	N/A	N/A	−47.266	−7.031	−33.203
h_3 (μm)	N/A	N/A	N/A	1.594	1.914
V_3 (V)	N/A	N/A	N/A	−35.938	33.594
h_4 (μm)	N/A	N/A	N/A	N/A	2.008
V_4 (V)	N/A	N/A	N/A	N/A	−30.469
e-beam diameter (μm)	65.126	10.038	9.223	9.082	8.873

Table 3. Optimized structural and electrical parameters with the gradient-based method.

	Double-gate type	Triple-gate type	Quadruple-gate type	Quintuple-gate type
h_1 (μm)	2.227	3.0	2.196	2.294
V_1 (V)	50.0	50.0	12.387	10.612
h_2 (μm)	N/A	2.0	2.100	2.0
V_2 (V)	N/A	−44.393	−15.769	−8.263
h_3 (μm)	N/A	N/A	2.281	2.256
V_3 (V)	N/A	N/A	−23.903	−11.759
h_4 (μm)	N/A	N/A	N/A	2.257
V_4 (V)	N/A	N/A	N/A	−15.934
e-beam diameter (μm)	10.647	10.180	11.125	9.535
Compared with GA (%)	−6.07	−10.38	−22.50	−7.46

for $N_C = 20$, the converged results show 14.3% and 11.2% increasing the e-beam diameter. Thus, we can conclude that the optimized results using the population size $N_C = 40$ is acceptable in general in considering the minor difference from those using $N_C = 100$.

4. Conclusion

In summary, we have introduced a GA into electron optics and demonstrated the use of GA as an intelligent approach to the design of the integrated FE devices for example. By means of combing parallel processing of the GA with field-emission simulation, we could optimize the e-beam focusability for double-gate, triple-gate, quadruple-gate and quintuple-gate FE devices by GA. With the judicious choice of location and bias of the focusing gates automatically extracted by GA, we are able to design the FE device with the smallest e-beam diameter at the anode. It is also noteworthy that the quintuple-gate type has the best focusability (e-beam diameter of 8.873 μm), while a triple-gate type can provide an acceptable focusability (e-beam diameter of 9.223 μm) considering manufacturability. Finally, the proposed optimization technique using a GA may be applied to optimize the e-beam performance in various electron-optical systems, including micro- and nanofabrication processes (i.e. parallel electron-beam lithography), electron microscope imaging for material science, displays and lighting (i.e. field-emission pixels), and accelerator physics.

Acknowledgments

The authors acknowledge C Chiu of the Department of Engineering Physics, Queen's University, Canada and Professor C T Sun of the Department of Computer Science and Information Engineering, National Chiao-Tung University, Taiwan for helping to develop the physical modeling and implementation of the PC cluster. We would also like to thank Drs J-H Tsai, T-C Cheng and M-P Lu of the National Nano-Device Laboratory, Taiwan for technical support and fruitful discussions. This work is funded by the National Nano-Device Laboratory, Taiwan.

References

[1] Milne M I, Teo K B K, Amaratunga G A J, Legagneux P, Gangloff L, Schnell J P, Semet V, Thien Binh V and Groening O 2004 *J. Mater. Chem.* **14** 933
[2] Iijima S 1991 *Nature* **354** 56
[3] Rinzler A G, Hafner J H, Nikolaev P, Lou L, Kim S G, Tomanek D, Nordlander P, Colbert D T and Smalley R E 1995 *Science* **270** 1179
[4] Liu P, Liu L, Wei Y, Sheng L and Fan S 2006 *Appl. Phys. Lett.* **89** 073101
[5] Patil A, Ohashi T, Buldum A and Dai L 2007 *Appl. Phys. Lett.* **89** 103103
[6] Choi J H *et al* 2005 *IEEE Trans. Electron Devices* **52** 2584
[7] Choi J H *et al* 2004 *Appl. Phys. Lett.* **84** 1022
[8] Choi Y S *et al* 2003 *Appl. Phys. Lett.* **82** 3565
[9] Oh T S, Yoo J B, Park C Y, Lee S E, Lee J H and Kim J M 2005 *J. Appl. Phys.* **98** 084313
[10] Xie C 2004 *IEEE Nanotechnol.* **3** 404
[11] Bae S, Seo W J, Choi S, Lee S and Koh K H 2004 *J. Vac. Sci. Technol.* B **22** 1303
[12] Hu Y and Lin T C 2006 *J. Vac. Sci. Technol.* B **24** 903
[13] Mammana V P and Fonseca L R C 2004 *Appl. Phys. Lett.* **85** 834
[14] Wei L, Zhang X, Yang G and Xie M 2006 *J. Vac. Sci. Technol.* B **24** 962

[15] Garner D M 2004 *J. Vac. Sci. Technol.* B **22** 1250
[16] Holland J 1975 *Adaptation in Nature and Artificial System* (Ann Arbor, MI: University of Michigan Press)
[17] Johnson J M and Rahmat-Samii Y 1997 *IEEE Antennas Propag. Mag.* **39** 7
[18] Hakansson A, Cervera F and Sanchez-Dehesa J 2005 *Appl. Phys. Lett.* **86** 054102
[19] Fujisawa T, Saitoh K, Wasa K and Koshiba M 2006 *Opt. Express* **14** 893
[20] Rinne J W and Wiltzius P 2006 *Opt. Express* **14** 9909
[21] Li Y 2007 *Microelectron. Eng.* **84** 260
[22] Dvorson L and Akinwande A I 2002 *J. Vac. Sci. Technol.* B **20** 53
[23] Jin J 2002 *Finite Element Method in Electromagnetics* (New York: Wiley)
[24] Amari S 2000 *IEEE Trans. Microw. Theory Technol.* **48** 1559
[25] Kozakowski P 2002 *IEEE Microw. Wireless Compon. Lett.* **12** 389